Silicide formation at the Ti/Si(111) interface: Diffusion parameters and behavior at elevated temperatures

S. A. Chambers, D. M. Hill, F. Xu, and J. H. Weaver
Department of Chemical Engineering and Materials Science, University of Minnesota, Minneapolis, Minnesota 55455
(Received 28 July 1986)

We have used high-resolution x-ray photoelectron spectroscopy to investigate the kinetics of formation of the Ti/Si(111)-7×7 interface as a function of temperature. At room temperature, we observe chemically shifted Si $2p$ core levels at binding energies of -0.6 and -1.1 eV relative to the substrate, corresponding to the formation of TiSi and Si in solution in Ti. When the temperature is increased ($T \lesssim 340$ °C), the rate of Ti diffusion through the TiSi layer to the Si substrate increases, more Si is released from the substrate, and Si is better able to out-diffuse into the Ti overlayer. There is then heterogeneous TiSi growth, together with diffusion of Si along grain boundaries to the surface. Measurements of the Si and Ti core-level emission as a function of time and temperature for 100-Å-thick Ti overlayers on Si(111) make it possible to determine lower limits for the effective diffusion coefficients and an upper limit for the effective activation energy for this process. By using Fick's second law with simplified boundary conditions, we found values of $(7.5\pm2.5)\times10^{-17}$ and $(7.5\pm2.5)\times10^{-16}$ cm^2/sec for the diffusion coefficient at 275 °C and 340 °C, respectively, and an activation energy of 24±9 kcal/mol (1.0±0.4 eV/atom).

The interfacial region formed when metal atoms are deposited onto semiconductor surfaces can be complex, heterogeneous, and metastable.[1–4] It is therefore important to understand the parameters which control its formation. Further, the morphology, atomic distribution, and chemical nature of the interface influence its interaction with its environment, as has been shown by observations of enhanced reactivity and interdiffusion.[1–15]

Although there have been extensive studies of room-temperature formation, there have been fewer studies of interface kinetics or behavior at elevated temperature. Central issues in interface dynamics include the mechanisms for substrate disruption and reaction, the stability of the reaction product, the ability of the reaction product to withstand large concentration gradients, and the role of crystallinity or grain boundaries in determining diffusion. Indeed, it is thought that grain boundaries provide paths for easy diffusion of metal and semiconductor atoms, thereby enhancing compound formation.

In this paper, we show that x-ray photoemission spectroscopy (XPS) can be used to determine the diffusion parameters at an interface. We do this by investigating the chemistry of formation of a refractory metal silicide at elevated temperature. In particular, we deposited relatively thick overlayers of Ti on Si and measured the rate of growth of the Si content of the overlayer as a function of time and temperature. This process can then be modeled with Fick's laws to obtain the diffusion coefficients at two temperatures and the activation energy E_a. We have chosen the Ti/Si(111) interface because this system has been studied by a variety of complementary techniques and there is a good base of information upon which to build. In particular, interface formation has been studied by Auger-electron spectroscopy,[11,12] medium-energy ion scattering,[14,15] valence-band photoemission,[11] high-resolution synchrotron-radiation core-level photoemission,[10] Rutherford backscattering spectroscopy,[16] glancing-angle x-ray diffraction,[16] transmission electron microscopy (TEM),[11] and Schottky-barrier-height measurements.[16] Although the emphasis of this paper is on Ti/Si, the technique used and the modeling should be applicable to other solid/solid interfaces where interdiffusion occurs.

All measurements were done with a Surface Science Instruments (SSI) SSX-100-03 x-ray photoelectron spectrometer appended to a dual chamber vacuum system designed for interface research.[2] Each system was separately pumped with 270 l/s noble-ion pumps, and a 4-in. gate valve isolated the preparation chamber from the measurement chamber. Sample introduction was done through the preparation chamber to keep the measurement chamber under UHV conditions at all times. The preparation chamber also served as a evaporation chamber so that extensive degassing of the metal source could be done prior to the measurements, in parallel with sample preparation procedures. The operating pressure was 4×10^{-11} Torr in both chambers. Sputtering of the silicon surface was done in the measurement chamber, and a cryopump provided rapid return of the system to base pressure. Photoelectrons were excited by monochromatrized Al k_α x-rays with photon beam diameters between 150 μm and 1 mm. The photoelectrons were energy analyzed with the SSI hemispherical analyzer at pass energies between 25 and 150 eV. The best energy resolution to date correspond to 0.45 eV full width at half maximum (FWHM) for the Si $2p_{3/2}$ core level. Data acquisition was facilitated by a multichannel detector with 128 parallel lines interfaced to a dedicated HP 9835C computer. Spectra could be collected for angles between grazing emission and normal emission. The half angle of acceptance of the

analyzer was 15°.

A Si wafer oriented to with 0.5° of (111) was chemically etched, Ar-ion sputtered, and annealed at 1000 °C to give a clean, reconstructed 7×7 surface. The carbon level was below the detection limit of XPS. Ti was evaporated from a Ta boat at pressures less than 2×10^{-10} Torr. The evaporation rate was monitored by a quartz-crystal oscillator (sample to source distance approximately 30 cm, rate between 1 and 5 Å per minute, Ti flux directed from the preparation chamber into the measurement chamber with no pumping impedance). No carbon or oxygen was detected on the sample surface immediately after Ti evaporation or after the kinetic runs at elevated temperature. The sample temperature was determined with an infrared pyrometer which had been calibrated with a thermocouple (accuracy ±15 °C).

In Fig. 1 we show Si $2p$ spectra collected for the clean surface and for the Ti/Si interface in various stages of its development. For these measurements, the photon energy was 1486.6 eV, the photoelectron kinetic energy was ~1385 eV, and the photoelectron mean free path was ~32 Å (as judged by the rate of attenuation of the substrate Si $2p$ peak with coverage). As a result, the measurements probe the outermost ~100 Å of the sample at normal emission, complementing the recent surface sensitive synchrotron radiation photoemission results of del Giudice *et al.*[10] The data of Fig. 1 were collected at a take-off angle of 90° (normal emission) using a 150-μm x-ray beam diameter and a 25-eV pass energy. The raw data are shown on the left-hand side, and representative core-level decompositions are shown on the right-hand side.

In the decomposition of the XPS spectra we fitted each experimental spectrum with pairs of functions of 70% Gaussian and 30% Lorentzian character corresponding to the spin-orbit-split $2p_{1/2}$ and $2p_{3/2}$ core levels. For each

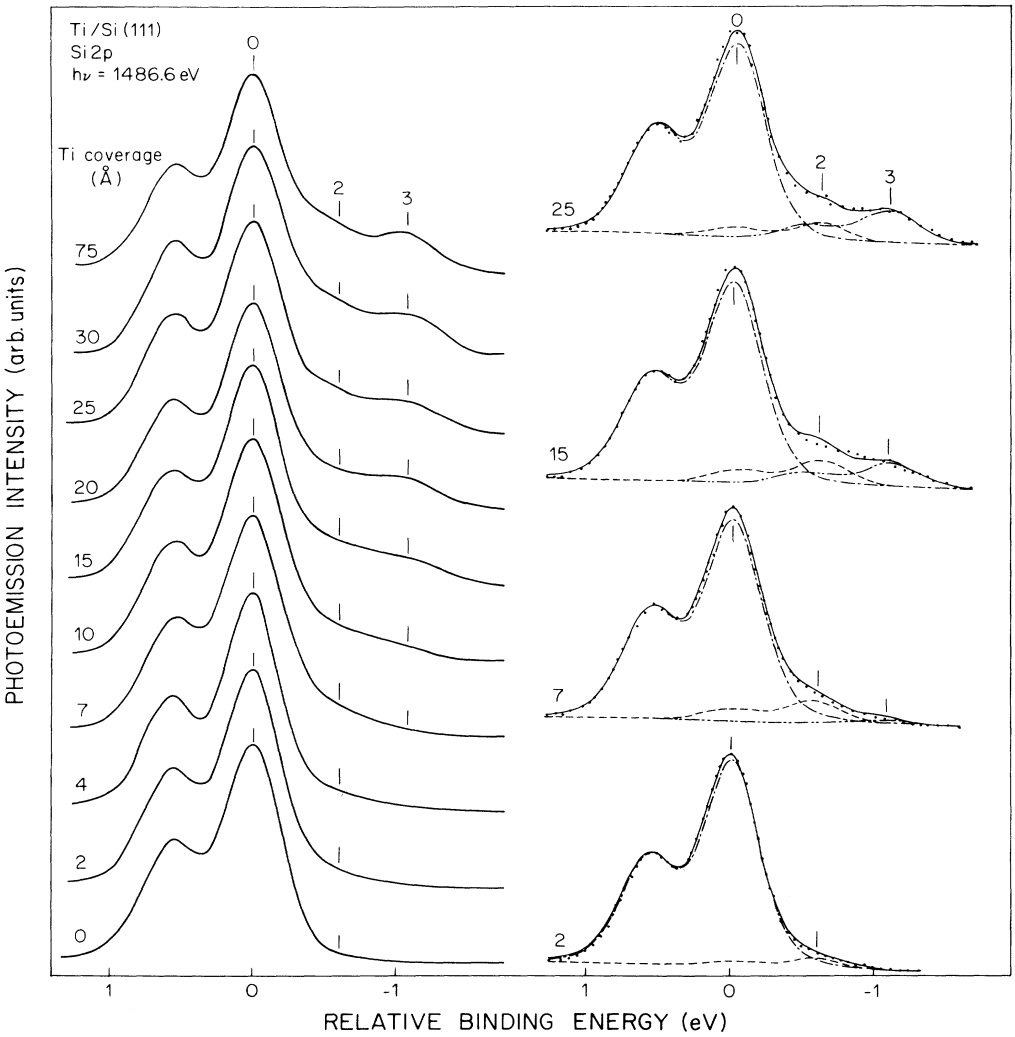

FIG. 1. High-resolution XPS Si $2p$ spectra of the evolving Ti/Si(111)-7×7 interface (left) and representative decompostions (right). The fitting curve in each case was a pair of functions of 70% Gaussian and 30% Lorentzian character. The spectra have been normalized to constant intensity for the purpose of comparison.

doublet the splitting was held to be 0.58 eV and the FWHM of each component was 0.45 eV. The branching ratio of the spin-orbit components was held constant at 1.93, the value obtained from normal emission spectra for the clean Si(111)-7×7 surface (see bottom left curve of Fig. 1). In doing the decomposition, the energy separations between the substrate and the two reacted components were held at 0.6 and 1.1 eV, as discussed by del Giudice *et al.*[10] The difference between the present XPS results and the synchrotron radiation results is that they had better overall resolution, and a more detailed decomposition could be done. In particular, they were able to observe a very small first component which we could not identify shifted by 0.35 eV, to detect changes in the width of component two, and to see a 125-meV shift in the final component. We adopt the notation of that paper in discussing the reaction products, even though the ultrathin region corresponding to number 1 is not resolved in the XPS results at room temperature.

The results of Fig. 1 show a reacted Si 2*p* component shifted 0.6 eV to lower binding energy relative to that of the substrate when the nominal Ti coverage reaches ~2 Å (labeled 2 in Fig. 1). The relative intensity of this feature grows with coverage until ~7 Å. Another reacted component (labeled 3) appears 1.1 eV below that of the substrate and amounts to 2% of the total signal by 7-Å coverage. This component grows in intensity until ~20-Å coverage but then diminishes as emission from each Si species in the interfacial region is attenuated by the growing metal overlayer. These observations agree with those of del Giudice *et al.*,[10] with differences related to the photoelectron mean free path, and we can use their modeling to assign the feature at −0.6 eV to TiSi and that at −1.1 eV to the solid solution phase of Si in Ti.

Reactive metal/semiconductor interfaces are known to form relatively thin reacted regions at room temperature. These are metastable since diffusion is a limiting factor in overlayer growth and is a thermally activated process. In our case here, the TiSi product is fully formed at room temperature by the deposition of ~15 Å of Ti, indicating that the polycrystalline TiSi layer is a good barrier against extensive intermixing and self-limits its own growth. Nevertheless, the temperature required to transform a thick Ti overlayer into the monosilicide phase is known to be considerably lower than that normally required for refractory metal silicide formation.[13] It has been proposed that this lower activation energy and the higher rate of silicide formation can be related to diffusion through grain boundaries in the TiSi barrier and in the evolving polycrystalline Ti overlayer. To investigate this phenomenon and to determine the kinetic parameters at the Ti/Si interface, we have performed real-time XPS measurements of the rate of change of the Si 2*p* and Ti 2*p* emission within the XPS probing depth (three times the mean free path or ~100 Å for Si 2*p* photoelectrons). These data can be used to determine the effective diffusion coefficient and activation energy for the early stages of formation based on Fick's law of diffusion.

In Fig. 2 we plot the integrated Si and Ti 2*p* intensities as a function of time for Ti/Si(111) interfaces prepared by the deposition of 100 Å of Ti at room temperature. The

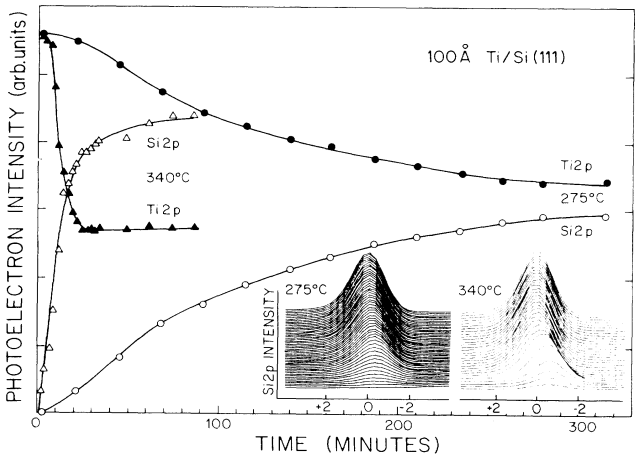

FIG. 2. Integrated Ti 2*p* and Si 2*p* intensities versus time for a 100-Å Ti overlayer on Si(111)-7×7 maintained at 275 and 340 °C. The uncertainty in each temperature is 15 °C. The insets show the time evolution of the Si 2*p* EDC's. The zero in binding energy for each family of spectra has been aligned with the peak position after equilibrium has been reached, not that of the Si substrate. The total binding-energy shift is 0.55±0.02 eV and 0.66±0.02 eV for the runs at 275 °C and 340 °C, respectively.

measurements were conducted at 275 and 340 °C and show the rapid appearance of Si in the probed region. Also shown are families of Si 2*p* spectra; the one in front was taken at the earliest time, and the interval between consecutive spectra was 2.5 and 4.7 min at 340 and 275 °C, respectively. These spectra were obtained at lower resolution than those shown in Fig. 1 to increase the rate of data acquisition (1-mm x-ray beam diameter and 150-eV pass energy). At thickness of 100 Å was chosen because this reduced the starting concentration of Si in the probed region below the level of detectability at room temperature (there was no evidence for Si surface segregation). As shown, the Si 2*p* intensity increased and the Ti 2*p* intensity decreased with increasing time due to atomic intermixing, and equilibrium was reached much more quickly for the interface held at 340 °C than for the one held at 275 °C. Moreover, the rate of Si out-diffusion dropped to zero at nearly the same time as did the rate of Ti indiffusion. The XPS results show that the final average composition of the interface formed at 340 °C was richer in Si than that formed at 275 °C. The experiment at 275 °C was run for 20 h, and both Si and Ti 2*p* intensities effectively plateaued by 325 min, indicating the formation of a metastable configuration.

The results of Fig. 2 show that the Si 2*p* core level shifts to higher binding energy as the overlayer became richer in Si. From its first appearance until the time equilibrium was reached, the center of the peak shifted by 0.55±0.02 eV and 0.66±0.02 eV for the runs at 275 °C and 340 °C, respectively, corresponding to the transformation from a Ti-rich environment about the emitting Si atoms to a more Si-rich environment. The different equilibrium stoichiometries and total core-level shifts at

the two temperatures demonstrate that the final average configuration formed at 275 °C is poorer in Si than that formed at 340 °C. The probed region is probably composed of incompletely reacted regions of Ti (containing Si) in a TiSi matrix.

In order to investigate the chemical nature of the interface once the interface formation reaction had ceased, we obtained high-resolution Si $2p$ spectra (150-μm x-ray beam diameter and 25-eV pass energy). In Fig. 3 we show the Si $2p$ spectra obtained at the completion of the 340 °C diffusion experiment after the sample had returned to room temperature. For comparison, we also show a spectrum obtained when 50 Å of Ti was deposited onto the sample at room temperature (top curve). This 50-Å spectrum shows three distinct chemical environments for Si atoms in the interfacial region, namely Si in the substrate, TiSi, and Si in solution in Ti. At room temperature, the substrate contribution is dominant because the reacted region is thin[10] and the photoelectron mean free path is large. [These spectra are normalized to give approximately constant heights for visual clarity, but intensity considerations show that the energy distribution curve (EDC) at 50 Å has been attenuated by a factor of about 70% relative to the clean surface.] Comparison of the room-temperature results and the annealed results shows that the largest component present after annealing corresponds to TiSi. There is no evidence of the solution phase, and we conclude that the overlayer is effectively TiSi. At the same time, Si is present in small amounts in two other chemical environments. The high binding-energy peak occurs at the same energy at the substrate peak, and the feature labeled 1 corresponds to that reported by del Giudice *et al.* at very low coverage. The appearance of Si $2p$ emission at the same binding energy as Si in the substrate may result from phase segregation upon cooling to room temperature or from uneven coverage of the substrate caused by substantial atomic redistribution during compound formation. Indeed, dark-field TEM micrographs by Butz *et al.*[11] showed that a 100-Å Ti film annealed at 300 °C for 20 min produces very small grains (10—50 Å) of silicide on the surface.

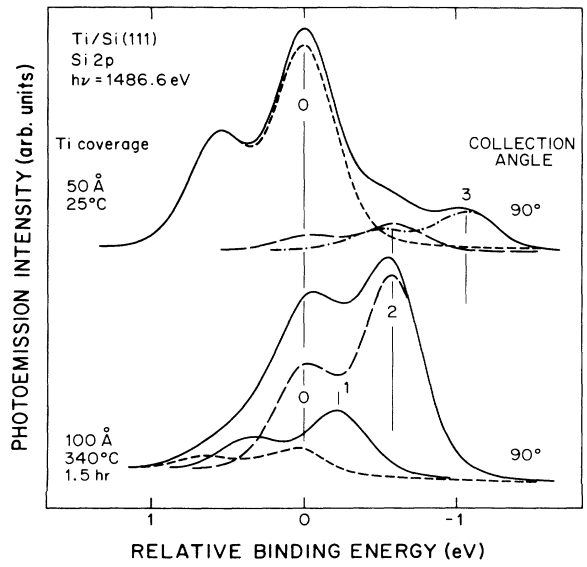

FIG. 3. High-resolution Si $2p$ spectra before and after annealing the Ti overlayer at 340 °C. Note that the Si $2p$ peaks were completely attenuated at 100 Å for the room-temperature interface. Chemical shifts observed with the 50-Å coverage are used to identify the phases present after annealing.

The evolution of the interface can be understood qualitatively by considering continued reaction induced by mass transfer. At room temperature a TiSi layer is known to form, sealing the substrate against extensive reaction when it coalesces, but also producing grain boundaries. These grain boundaries provide the primary channels for Ti and Si diffusion through the TiSi barrier. The indiffusion of Ti to the Si substrate increases exponentially with temperature and provides for the continued disruption of the substrate. This facilitates the release of Si into those same channels. When Si reaches the Ti-rich overlayer, it is able to react with Ti to form TiSi, when the local concentration of Si is adequate, but it also is able to out-diffuse through grains of the Ti. This explains why we first observe Si in the "solution" phase. In time, however, the active grain boundaries in the Ti are modified by TiSi formation and the extent of the TiSi region grows. For such a system, the dynamics of mass transfer are time dependent because the morphology of the overlayer is itself time dependent. This is consistent with the results shown in Figs. 2 and 3.

The results shown in Fig. 2 for the early stages of intermixing make it possible to extract diffusion parameters for Si moving into the the interfacial region during the very early stages of the process, i.e., before the morphology of the overlayer has changed too drastically by the growth of TiSi in the Ti grain boundaries. The mathematics of diffusion with boundary conditions appropriate for thin films has been treated in detail elsewhere.[17] Different solutions to Fick's second law have been proposed which involve some combination of grain boundary and lattice diffusion, and concentration profiles have been determined. The resulting solutions tend to be mathematically complex and involve measurements such as autoradiography or Auger-ion sputter profiling to determine the spatial distribution of the diffusing species. In what follows, we outline a considerably simpler method to extract diffusion parameters from dynamic, nondestructive XPS measurements. Details of the derivation can be found in the Appendix.

The general solution to Fick's second law for diffusion in one dimension,

$$\frac{\partial c(x,t)}{\partial t} = D\frac{\partial^2 c(x,t)}{\partial x^2} , \tag{1}$$

is given by

$$c(x,t) = (A/\sqrt{t})\exp(-x^2/4Dt) , \tag{2}$$

where D is the diffusion coefficient and A is a constant of integration. For the system under consideration here, the diffusion coefficient and the activation energy that we will determine will be effective values applicable to the system composed of the Si substrate, a polycrystalline

TiSi interlayer, and a polycrystalline Ti overlayer. The values for both the diffusion coefficient and the activation energy can be safely assumed to be upper limits because an unknown fraction of the out-diffused Si will be chemically trapped in the grain boundaries. The essential boundary condition is that for times less than that required for the advancing Si to reach the surface, the overlayer can be treated as being infinitely thick. The use of a one-dimensional model is justified because all grain boundaries which promote Si diffusion into the overlayer have a component normal to the interface and our 1-mm diameter x-ray beam irradiates a large number of grain boundaries.

If we define M as the amount of Si per unit cross-section area at the interface and x as the direction normal to the interface, we can evaluate the constant A under the above boundary condition to give

$$c(x,t)=(M/2\sqrt{\pi Dt})\exp(-x^2/4Dt)\ . \tag{3}$$

Integrating over all cross-sectional areas, we obtained for the Si concentration

$$c(x,t)=(c'/2)[1-\mathrm{erf}(x/2\sqrt{Dt})]\ , \tag{4}$$

where x is zero at the Si interface and increases toward the surface, and c' is the Si concentration in the substrate. We then can relate the average Si concentration in the overlayer to the associated photoelectron intensity $I(t)$ by the relation

$$I(t)\propto\int_{h-3\lambda}^{h}c(x,t)\exp[-(h-x)/\lambda]dx=(c'/2)\int_{h-3\lambda}^{h}[1-\mathrm{erf}(x/2\sqrt{Dt})]\exp[-(h-x)/\lambda]dx\ , \tag{5}$$

where λ is the inelastic mean free path for Si $2p$ emission and h is the overlayer thickness. The constant of proportionality is dependent on the photoelectron cross section and the instrument response function. In order to evaluate the integral of Eq. (5) we must first relate c' to the intensity from the clean substrate under the same conditions as those used in the kinetics experiments. Doing so yields $c'\propto(I'/\lambda)$, where the constant of proportionality is the same as that found in Eq. (5). Therefore, this constant cancels out of the expression. In doing the experiment, we deliberately picked h to be nearly equal to 3λ to simplify the expression as much as possible. Making this substitution, we arrive at

$$I(t)/I'=\left[\frac{1}{2\lambda}\right]\int_0^h[1-\mathrm{erf}(x/2\sqrt{Dt})]\times\exp[-(h-x)/\lambda]dx\ , \tag{6}$$

which can be integrated numerically for different choices of D and compared to experiment.

In Fig. 4 we show a comparison of the measured Si $2p$ photoelectron intensity and that calculated using Eq. (6). Different values of D have been assumed in the calculation, as shown. The boundary conditions used to derive Eq. (6) are appropriate only for the first few data points in each case (i.e., those times for which it is least likely that Si atoms have reached the surface), and we attempt to fit the model to experiment only for the first five data points. For the results at 275 °C, the experimental data points are bracketed by predicted curves obtained with $D=5\times10^{-17}$ and 1×10^{-16} cm^2/sec, leading to a value of $7.5\pm2.5\times10^{-17}$ cm^2/sec. Similarly, experimental results at 340 °C are bracketed between $D=5\times10^{-16}$ and 1×10^{-15} cm^2/sec, leading to a value of $7.5\pm2.5\times10^{-16}$ cm^2/sec. These diffusion coefficients may then be used to determine the activation energy E_a and preexponential factor D_0. Employing the Arrhenius equation, we find $E_a=24$ kcal/mol (1.0 eV/atom) and $D_0=2.8\times10^{-7}$ cm^2/sec. With propagation-of-errors theory, we can calculate the derived uncertainties in E_a and D_0 to obtain $\delta E_a=9$ kcal/mol (0.4 eV/atom) and $\delta D_0=2\times10^{-6}$ cm^2/sec. Unfortunately, since δD_0 is seven times larger than D_0 we conclude that the preexponential factor cannot be determined reliably when only two values of the diffusion coefficient are known and the uncertainty in each is $\sim30\%$.

Our description of the annealed interface is consistent with that of Rubloff and co-workers[13,15] who used medium-energy ion scattering to determine the composition of the overlayer after brief anneals. Those authors concluded that annealing at a temperature of 500 °C converts the interface to a TiSi phase. Moreover, they concluded that the ion scattering spectra at lower annealing

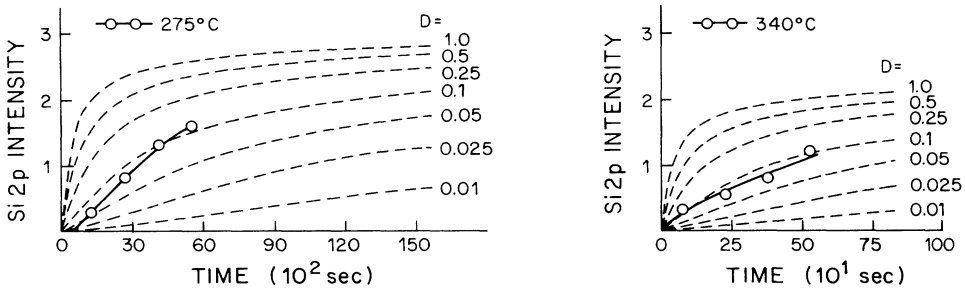

FIG. 4. Fits of the first several data points from Fig. 2 to model intensity curves based on a solution to Fick's second law. Only the first several data points were fit in order to satisfy the boundary conditions used to obtain the solution (see text). The units of D are 10^{-15} cm^2/sec and 10^{-14} cm^2/sec for the fits to data collected at 275 °C and 340 °C, respectively.

temperatures are represented by a weighted average of spectra of the unannealed and reacted TiSi interfaces. Our results show that there is also a Si-in-Ti solution phase, that its spatial extent varies with temperature, and that extensive conversion to TiSi has occurred after 1.5 h at 340 °C. Studies at temperatures of ~750 °C have shown that this TiSi phase will ultimately convert to $TiSi_2$, becoming chemically homogeneous.[11,16]

ACKNOWLEDGMENTS

We are pleased to acknowledge stimulating discussions with Y. Shapira, M. del Giudice, R. A. Butera, and D.A. Shores. This work was supported by Office of Naval Research Contract No. N00014-86-K-0427.

APPENDIX

By inspection, the general solution to the one-dimensional expression of Fick's second law,

$$\frac{\partial c(x,t)}{\partial t}=D\frac{\partial^2 c(x,t)}{\partial x^2} \tag{A1}$$

is given by,

$$c(x,t)=(A/\sqrt{t})\exp(-x^2/4Dt)\ , \tag{A2}$$

where $c(x,t)$ is the concentration of the diffusing species at point x and time t, D is the diffusion coefficient, and A is a constant of integration. Defining M as the total mass of diffusing species per unit cross-sectional area normal to the direction of motion (x), A can be evaluated by integrating $c(x,t)$ over all x and setting the result equal to M:

$$M=\int_{-\infty}^{\infty} c(x,t)dx$$
$$=(A/\sqrt{t})\int_{-\infty}^{\infty}\exp(-x^2/4Dt)dx=2A\sqrt{\pi D}\ . \tag{A3}$$

Therefore,

$$A=M/2\sqrt{\pi D}\ . \tag{A4}$$

We then assume that $c(x,t)$ is a step function at $t=0$ defined as

$$c(x,0)=\begin{cases} c' & \text{for } x\geq 0 \\ 0 & \text{for } x<0\ , \end{cases}$$

where the origin is at the interface plane, positive x is defined to be in the direction of the substrate, and c' is the Si (solute) concentration within the substrate. The contribution to $c(x,t)$ due to an infinitesimally thin slab of solute centered at $x=x_i$ and with thickness dx is given by

$$c_i(x,t)=(c'dx/2\sqrt{\pi Dt})\exp[-(x-x_i)^2/4Dt]\ . \tag{A5}$$

The total distribution function is obtained by integrating Eq. (5) over all slabs of solute

$$c(x,t)=\int_0^{\infty} c_i(x,t)dx$$
$$=(c'/2\sqrt{\pi Dt})\int_0^{\infty}\exp[-(x-x_i)^2/4Dt]dx\ . \tag{A6}$$

Introducing a change of variables, $\phi\equiv(x-x_i)/2\sqrt{Dt}$, Eq. (6) becomes

$$c(x,t)=(c'/\sqrt{\pi})\int_{-\infty}^{x/2\sqrt{Dt}}\exp(-\phi^2)d\phi$$
$$=(c'/2)[1+\mathrm{erf}(x/2\sqrt{Dt})]\ . \tag{A7}$$

Redefining our coordinate system so that positive x extends into the overlayer rather than into the substrate, we get

$$c(x,t)=(c'/2)[1-\mathrm{erf}(x/2\sqrt{Dt})]\ . \tag{A8}$$

Next, we relate the instantaneous solute concentration $c(x,t)$ to the associated XPS intensity. If the overlayer thickness is h, the normal-emission XPS intensity from an infinitesimal volume element a distance x from the interface plane is given by

$$dI(x,t)\propto c(x,t)\exp[-(h-x)/\lambda]dx\ , \tag{A9}$$

where λ is the photoelectron inelastic mean free path. The constant of proportionality depends on the photoelectric cross section, the instrument transmission and the detector efficiency. Integrating from the surface (located at $x=h$) to a depth of 3λ below the surface accounts for 95% of the total intensity and yields

$$I(t)\propto -\int_h^{h-3\lambda} c(x,t)\exp[-(h-x)/\lambda]dx=-(c'/2)\int_h^{h-3\lambda}[1-\mathrm{erf}(x/2\sqrt{Dt})]\exp[-(h-x)/\lambda]dx\ . \tag{A10}$$

The solute concentration within the substrate, c', can be evaluated in terms of the solute photoelectron intensity from a sample of pure solute (I') by integrating the differential intensity from a volume element a distance x beneath the surface over all depths. In this integral only, we define $x=0$ as the surface plane and positive x as pointing into the bulk. The result is

$$I'\propto c'\int_0^{\infty}\exp(-x/\lambda)dx=c'\lambda\ . \tag{A11}$$

If we assume that the photoelectric cross section for solute emission is the same in the overlayer as in a pure specimen, the constant of proportionality in Eq. (11) is the same as that found in Eqs. (9) and (10). Under this assumption, insertion of Eq. (11) into Eq. (10) yields

$$I(t)/I'=-\left[\frac{1}{2\lambda}\right]\int_h^{h-3\lambda}[1-\mathrm{erf}(x/2\sqrt{Dt})]$$
$$\times\exp[-(h-x)/\lambda]dx\ . \tag{A12}$$

If h is picked to be $\sim 3\lambda$, the upper limit of integration becomes 0. Also, the minus sign can be removed from the expression by reversing the limits of integration. The final result is given by

$$I(t)/I'=\left[\frac{1}{2\lambda}\right]\int_0^{h}[1-\mathrm{erf}(x/2\sqrt{Dt})]$$
$$\times\exp[-(h-x)/\lambda]dx\ . \tag{A13}$$

[1]L. J. Brillson, Surf. Sci. Rep. **2**, 123 (1982).
[2]J. H. Weaver, Phys. Today **39**, 24 (1986). A photograph of the instrument used in these measurements appeared on the cover of the January issue.
[3]See, for example, *Thin Films-Interdiffusion and Reactions,* edited by J. M. Poate, K. N. Tu, and J. W. Mayer (Wiley, New York, 1978); G. Ottaviani, K. N. Tu, and J. W. Mayer, Phys. Rev. B **24**, 3354 (1981).
[4]J. H. Weaver, in *Analysis and Characterization of Thin Films,* edited by K. N. Tu and R. Rosenberg (Academic, New York, in press).
[5]A. Franciosi, J. H. Weaver, and D. G. O'Neill, Phys. Rev. B **28**, 4889 (1983); and J. Vac. Sci. Technol. B **1**, 524 (1983).
[6]A. Cros, J. Derrien, and F. Salvan, Surf. Sci. **110**, 471 (1981); A. Cros, F. Salvan, and J. Derrien, J. Appl. Phys. **52**, 4757 (1981).
[7]I. Abbati, G. Rossi, L. Calliari, L. Braicovich, I. Lindau, and W. E. Spicer, J. Vac. Sci. Technol. **21**, 409 (1982).
[8]S. Chang, A. Rizzi, C. Caprile, P. Philip, A. Wall, and A. Franciosi, J. Vac. Sci. Technol. A **4**, 799 (1986).
[9]R. A. Butera, M. del Giudice, and J. H. Weaver, Phys. Rev. B **33**, 5435 (1986).
[10]M. del Giudice, J. J. Joyce, M. W. Ruckman, and J. H. Weaver (unpublished).
[11]R. Butz, G. W. Rubloff, T. Y. Tan, and P. S. Ho, Phys. Rev. B **30**, 5421 (1984).
[12]L. J. Brillson, M. L. Shade, H. W. Richter, H. Vander Plas, and R. T. Fulks, Appl. Phys. Lett. **47**, 1080 (1985).
[13]G. W. Rubloff (unpublished).
[14]E. J. van Loenen, A. E. M. J. Fischer, and J. F. van der Veen, Surf. Sci. **155**, 65 (1985).
[15]R. M. Tromp, G. W. Rubloff, and E. J. van Loenen, J. Vac. Sci. Technol. A **4**, 865 (1986).
[16]M. O. Aboelfotoh and K. N. Tu, Phys. Rev. B **33**, 6572 (1986); **34**, 2311 (1986).
[17]D. Gupta, D. R. Campbell, and P. S. Ho, in *Thin Films-Interdiffusion and Reaction,* Ref. 3 above.